The Influence of Coastal Orography: The Yakutat Storm

JAMES E. OVERLAND

Pacific Marine Environmental Laboratory, National Oceanic and Atmospheric Administration, Seattle, Washington

NICHOLAS BOND

Joint Institute for the Study of Atmosphere and Ocean, University of Washington, Seattle, Washington

(Manuscript received 21 September 1992, in final form 9 November 1992)

ABSTRACT

An unforecast windstorm in the vicinity of Yakutat, Alaska, on 14 March 1979 illustrates the importance of ageostrophic dynamics within a coastal zone proximal to significant terrain. Large pressure rises [greater than 4 mb $(3\ h)^{-1}$] were observed along the southeastern Alaska coast after passage of a cold front when the low-level geostrophic flow was directed onshore. These pressure rises did not occur simultaneously along the coast, but rather propagated northward along the coast as a coherent pulse or surge. Strong surface winds (approximately 25–30 m s^{-1}) were observed in the region of large sea level pressure gradient at the leading edge of the surge and occurred after the passage of the synoptic front. Although the sparseness of the observations prevent definite conclusions, this feature resembles a Kelvin wave more than a density current. Omega dropwindsonde observations collected along the coast of Alaska during two other, less dramatic, situations suggest damming and downslope flow structures important to the interpretation of the Yakutat storm.

Coastal semigeostrophic dynamics, that is, an ageostrophic momentum balance in the alongshore direction, occurs when the coastal mountains are hydrodynamically steep. The steep regime is defined by the nondimensional slope $(h_m/l_m)(N/f) > 1$, where h_m is mountain height, l_m is mountain half-width, N is the static stability for the incident flow, and f is the Coriolis parameter. For typical values of $N \sim 10^{-2}\ s^{-1}$, the coast is wall-like when $h_m/l_m > 0.01$. Given a wall-like nature of the coast, trapped isolated mesoscale features, with an offshore length scale given by a Rossby radius of $O(100$ km), propagate alongshore ageostrophically due to a combination of Kelvin waves, density currents, or forced response. To correctly forecast in the coastal zone, numerical weather prediction models must qualitatively resolve terrain slopes so that the modeled dynamics are in the correct semigeostrophic or quasigeostrophic hydrodynamic regime.

1. Introduction and basic parameters

The transition from a nearly flat ocean to land in the coastal zone is often accompanied by major changes in elevation. Flow over and around such changes in orography in a rotating stratified fluid represents one of the classic problems in meteorology and oceanography. For a far-field wind perpendicular to a barrier one wishes to know the horizontal extent and magnitude of upstream modification of the flow pattern in response to the barrier. There is also a downwind modification of the flow that is not, in general, symmetric with the upwind influence. One is also interested in how a storm itself is modified by the presence of mountains (Schumann 1987).

Theories of upstream influence show that (Smith 1979) low-level flow is generally blocked by a mountain when the Froude number

$$\mathrm{Fr} = \frac{U}{h_m N} \tag{1}$$

is less than unity. Parameter N is the static stability $[(g/\theta_o)\partial\theta/\partial z]^{1/2}$, where θ_o is constant mean potential temperature, g is gravity, h_m is height of the ridge, and U is the speed of the free airstream. The flow response is complex, however (Smith 1989), and is not related simply to the ratio of the kinetic to the potential energy in (1). For typical atmospheric stratification of $N \approx 10^{-1}$–$10^{-2}\ s^{-1}$, elevation of only 100 m is often sufficient to cause blocking of the onshore flow at low levels. This "blocking" is a common occurrence along the west coast of the United States (e.g., Neiburger 1960); when it occurs along the East Coast it is often referred to as "cold-air damming." Leeside effects can be important for flow directed offshore. In the coastal zone it is not necessary to have an upstream velocity directed toward the mountains for the orography to influence coastal winds. If a localized region of high or low pressure is generated in the coastal zone it will, under certain conditions, be "trapped" and propagate along the coastline within the coastal zone. This is a

Corresponding author address: Dr. James E. Overland, Pacific Marine Environmental Laboratory, NOAA, Bldg. No. 3, 7600 Sand Point Way N.E., Seattle, WA 98115.

common phenomenon along the coasts of Australia, California, and Oregon.

The Froude number is a measure of the importance of vertical displacement of isentropic surfaces by an obstacle or ridge. A second factor is the influence of the earth's rotation on upstream flow deceleration (Queney 1948). One can consider the influence of rotation through a Rossby number,

$$R_m = \frac{U}{fl_m}, \tag{2}$$

where U is the upstream velocity, f is the Coriolis force, and l_m is the half-width of the ridge; little flow deceleration is found when R_m is less than unity. Numerical simulations by Pierrehumbert and Wyman (1985) and trajectory analyses by Chen and Smith (1987) suggest that in the region of steep orography the deceleration zone will grow upstream to a width of

$$l_R = \frac{Nh_m}{f}. \tag{3}$$

This parameter, l_R, is known as the radius of deformation. Xu (1990) alternately argues that the upstream width is also a function of the Froude number. Steep orography is defined by the nondimensional slope, $(h_m/l_m)(N/f)$, being greater than unity (Prandtl 1936; Burger 1991). For the coastal case l_R is often of order 50–150 km and $l_R > l_m$; this contrasts with broad mountain ranges such as the Rockies with l_m of order 500 km. In the broad mountain case, $l_m > l_R$, the flow stays quasigeostrophic with $R_m < 1$, that is, wind blows perpendicular to the pressure gradient as it flows over the orography, with little upstream influence. The coastal region, however, is often in the knife-edge mountain case, $l_R > l_m$, and $R_m \geq 1$. Here one expects the coastal mountains to represent a wall and that the momentum balance in the alongshore direction near the wall is not geostrophic. Current operational numerical weather prediction models have grids too coarse to resolve terrain slopes and thus do not correctly simulate coastal phenomena.

The effects of coastal terrain are illustrated with three case studies of the flow along the southern and southeastern Alaska coast. All three cases feature a synoptic low pressure center in the Gulf of Alaska. Our focus is on 14 March 1979 near Yakutat, Alaska, when marine forecasts called for winds up to 30 kt, and winds as great as 70 kt were reported. This case came to our attention from the angry letters sent by a fisherman who was caught by the storm. The other two cases of 26 April 1992 and 15 March 1985 are less dramatic, but feature Omega dropwindsonde (ODW) observations from a research aircraft. In the April case the low-level coastal flow in an offshore regime is compared with that in an onshore regime. The March case is distinguished by relatively dense ODW observations and shows the difficulty in separating the orographically induced motions from those inherent to the storm.

2. Scale analysis and classic examples

a. Equations of motion

To delineate the influence of orography on coastal meteorology, let L be the scale for motion in the alongcoast (y) direction and l be the scale in the offshore ($-x$) direction where $l_m < l < L$. We can nondimensionalize the equations of motion with velocities scaled by u, $v = V = UL/l$, time by l/U, vertical distances by $D = fl/N$, pressure p by $\rho_o flU$, and density by $\rho_o Nfl/g$; ρ_o is a constant mean density. The equations of motion for a shallow system are (Overland 1984; Pierrehumbert and Wyman 1985):

$$R_l\left(\frac{l}{L}\right)^2\left(\frac{du}{dt} + C'_D u\right) = v - \frac{\partial P_o}{\partial x} - \frac{\partial p}{\partial x} \quad \text{(cross-shore), and} \tag{4}$$

$$R_l\left(\frac{dv}{dt} + C'_D v\right) = -u - \frac{\partial P_o}{\partial y} - \frac{\partial p}{\partial y} \quad \text{(alongshore),} \tag{5}$$

with $R_l = U/fl = V/fL$, a coastal Rossby number, and $C'_D = C_D(U + V)/D$, a coastal drag coefficient which indicates the relative importance of surface friction. The term $\partial P_o/\partial y$ on the right-hand side of (5) nondimensionally equals unity and represents the alongshore pressure gradient associated with the incident geostrophic wind U. For many coastal problems the left-hand side of (4) is small even though R_l may be of $O(1)$; the flow in the alongshore direction is in geostrophic balance. The left-hand side of (5), however, is of $O(1)$ and v exhibits accelerations in response to the imposed alongshore pressure gradient. Small l/L and $R_l \sim 1$ yield the coastal zone semigeostrophic approximation. The only remaining free parameter is the nondimensional mountain height which introduces the stratification parameter N:

$$\frac{h_m}{D} = \frac{N}{f}\frac{h_m}{l}. \tag{6}$$

This may also be written as R_l/Fr. Thus the coastal mountain problem can be specified in terms of R_l and Fr, a Rossby number and a Froude number. Note that for $h_m/D = 1$, that is, steep orography, the offshore length scale obtained from (6) is $l = l_R$, the Rossby radius of deformation that scales coastal influence offshore of mountainous coasts as 50–150 km.

The foregoing discussion suggests that mesoscale meteorological features O(50–150 km) exist in the vicinity of coastal orography, and that an ageostrophic momentum balance is anticipated in the alongshore direction. However, the upstream flow is seldom stationary and uniform and vertical stratification is seldom

constant. While theoretical considerations define the scales and processes important to the coastal zone, they are less successful in fully explaining particular case studies (Walter and Overland 1982; Mass and Ferber 1990; National Research Council 1992).

b. *Examples of coastal flow: Damming, surges, and lee effects*

Here we discuss some previous observations of orographically induced structures along a mountain ridge to indicate the phenomena that are possibly important along the coast of southeastern Alaska.

During conditions of uniform onshore flow characterized by a low Froude number, the steady-state response to terrain is a coastal ridge, the phenomenon known as damming. The topographically induced pressure fields produce along-ridge pressure gradients that can result in barrier jets (e.g., Parish 1982). The best-documented cases of damming have been along the east coast of the Appalachian Mountains of the United States (Bell and Bosart 1988; Xu 1990; Doyle and Warner 1991). These episodes arise when there is high pressure over New England and onshore flow toward the Appalachians with an estimated Froude number of 0.3–0.4. When the incident flow is not uniform, notably in the vicinity of a storm, the same sort of structures can occur. Mass and Ferber (1990) show the development of ridging along the coast of western Washington state with the approach of a cold-frontal system. The ageostrophic response to the induced alongshore pressure gradients appears to have caused coastal winds stronger than the winds in the weather system when it was farther offshore. Similar supergeostrophic winds have been observed at coastal stations along Alaska (Reynolds 1983; Businger and Walter 1988).

The time-dependent aspects of low-Froude-number flows are illustrated by case studies of disturbances that form and propagate along mountainous coastlines. These mesoscale coastal features have been documented along California by Dorman (1985, 1987), Mass et al. (1986), Beardsley et al. (1987), Mass and Albright (1987), Zemba and Friehe (1987), Winant et al. (1988), and along Australia by Holland and Leslie (1986). Typically these cases feature strong temperature inversions below the height of the topography, and the static stability can be represented by the difference in potential temperature, $\theta_2 - \theta_1$, across the inversion occurring at height h_i. The coastal zone semigeostrophic equations admit Kelvin wave solutions

$$\frac{h_i'}{D} = e^{-|x|} G(y - t), \tag{7}$$

with G an arbitrary functional shape (Reason and Steyn 1990). The solution is trapped to a unit distance from the coast, that is, a Rossby radius, and propagates at a unit speed that in dimensional terms has the phase speed $c = fl_R$. On the other hand, if the equations are initialized with density front, a gravity current can form that is nonlinear. Alongshore disturbances can also be forced by an alongshore pressure gradient $\partial P_o/\partial y$ imposed by the synoptic-scale pressure field above the coastal layer. While these isolated wave–frontal features are perhaps the most obvious of coastal phenomena, understanding their source mechanisms and composite nature (density flow versus propagating wave) is uncertain. These isolated trapped phenomena are generally initiated by changes in the synoptic-scale flow.

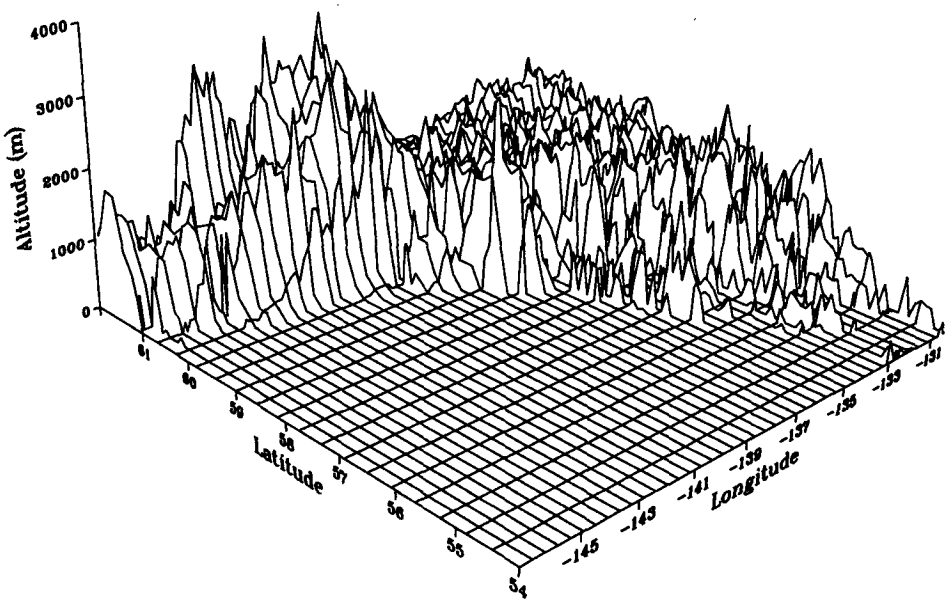

FIG. 1. Topography along the coastline of the northeastern portion of the Gulf of Alaska.

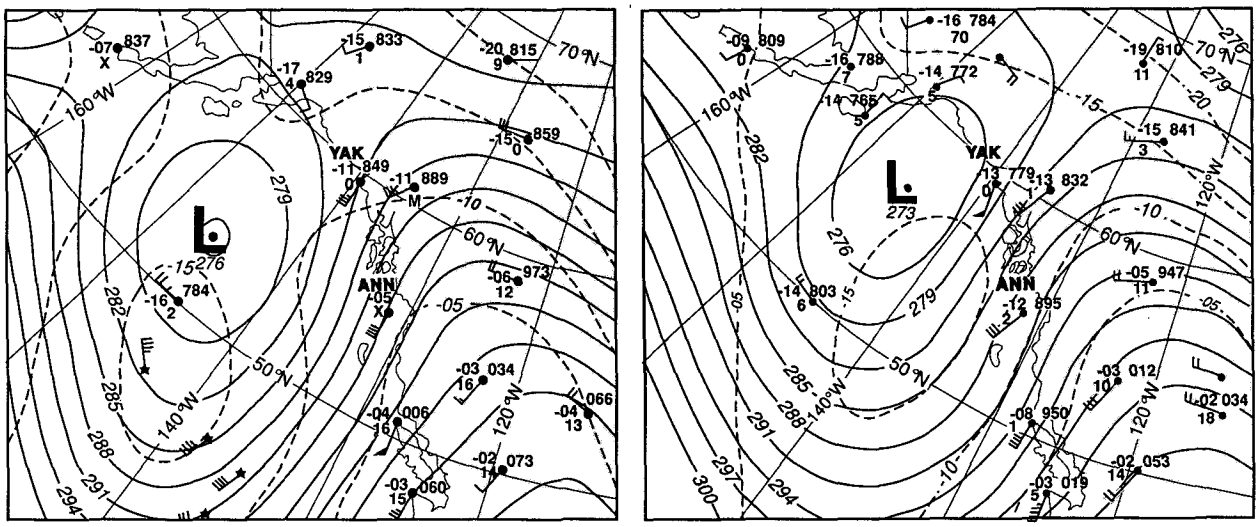

FIG. 2. (a) 700-mb analysis at 1200 UTC 14 March 1979 from the National Meteorological Center. (b) As in (a) but for 0000 UTC 15 March 1979.

The climatology of such changes is not well documented.

Lee effects from offshore flow are likely to be important at times along the Alaska coast. The lower-tropospheric flow (up to approximately 700 mb) is often directed offshore in the northern Gulf of Alaska as mature low pressure systems move into the region and decay. Because of the height and steepness of the terrain along the coast, the orography is narrow in a dynamical sense; the Alps and the mountains along the Adriatic coast of Yugoslavia represent better proxies for coastal Alaska than the Rockies. Enhanced downslope winds have been documented in southeastern Alaska with characteristics resembling other local downslope windstorms (Colman and Dierking 1992). A related but different type of phenomenon is lee cyclogenesis. Buzzi and Tibaldi (1978) analyzed a case of Alpine lee cyclogenesis in which the windward retardation of low-level cold air appeared to be crucial. There is some analogy to southeastern Alaska, where the coastal mountains during the cool season separate cold, continental air from the maritime air over the Gulf. The southeastern Alaska situation is further complicated by differential surface friction and diabatic heating over the water relative to the land.

3. The Yakutat storm of 14 March 1979

a. Description

Poor verification of coastal weather forecasts is often attributed to the formation of mesoscale systems by the interaction of storms with coastal orography and to the feedback of these features on storm intensity within the coastal zone (±100 km); yet even basic documentation of this interaction and feedback is lacking (Bane et al. 1990). In this section we discuss a case study that documents the influence of coastal orography on a landfalling storm. To the south of the landfalling point, Kelvin wave–like and damming phenomena were observed. North of the landfalling point, down-pressure-gradient offshore flow is suggested.

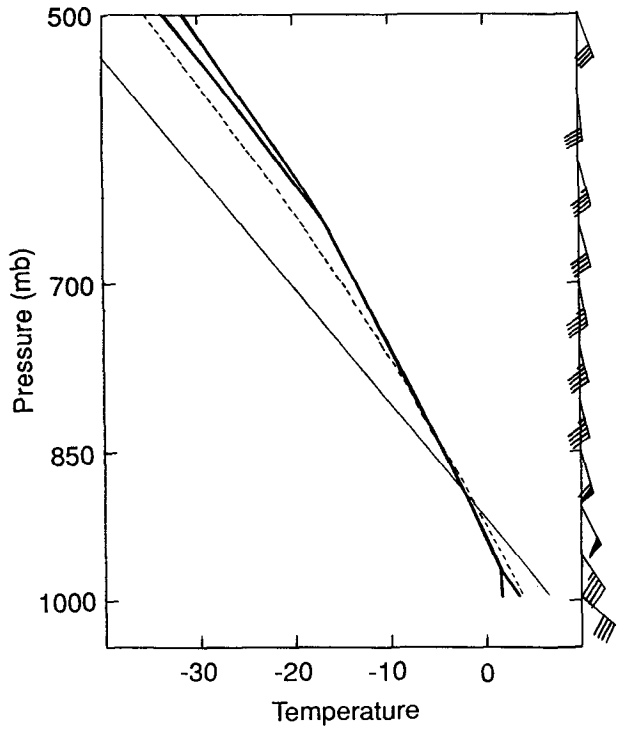

FIG. 3. Sounding from Yakutat, Alaska (YAK), at 0000 UTC 15 March 1979. The thick solid lines represent air temperature and dewpoint. Winds are plotted in the conventional manner (full barb is 5 m s^{-1}). The thin solid (dashed) line represents a surface of constant potential (equivalent potential) temperature.

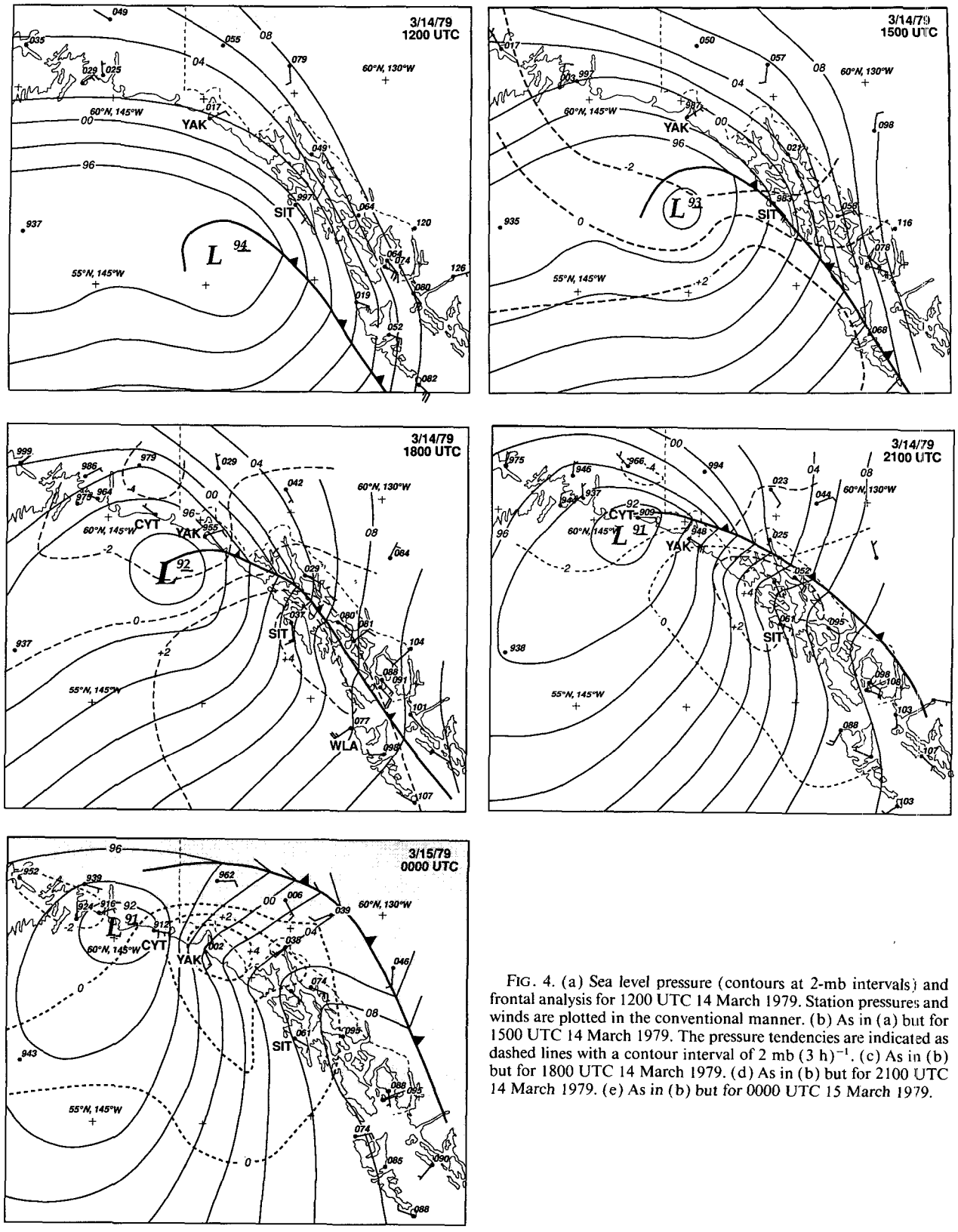

FIG. 4. (a) Sea level pressure (contours at 2-mb intervals) and frontal analysis for 1200 UTC 14 March 1979. Station pressures and winds are plotted in the conventional manner. (b) As in (a) but for 1500 UTC 14 March 1979. The pressure tendencies are indicated as dashed lines with a contour interval of 2 mb (3 h)$^{-1}$. (c) As in (b) but for 1800 UTC 14 March 1979. (d) As in (b) but for 2100 UTC 14 March 1979. (e) As in (b) but for 0000 UTC 15 March 1979.

The strongest winds reported at Yakutat were at 2100–2200 UTC 14 March 1979; analysis is provided for the period between 1200 UTC on the 14th and 0000 UTC on the 15th. A perspective view of the coastal terrain in the region of interest is shown in Fig. 1.

The 700-mb analysis at 1200 UTC 14 March 1979 (Fig. 2a) from the National Meteorological Center (NMC) shows a midtropospheric circulation dominated by a low centered near 53°N, 145°W. The 700-mb winds were directed mostly alongshore and slightly onshore along the southern and southeastern Alaskan coast. The thermal gradient between Yakutat (YAK) and Annette (ANN) implies that the southwesterly component of the geostrophic flow was decreasing toward the surface. Strong cold-air advection is shown in a baroclinic zone southeast of the low center within a band roughly 200–500 km offshore. As will be shown below, the surface front associated with this baroclinic zone moved onshore between 1500 and 1800 UTC. The 700-mb analysis at 0000 UTC 15 March (Fig. 2b) shows that the low center had deepened by 30 m and moved approximately 300 km northward in the previous 12 hours. The 700-mb flow along the southeastern Alaskan coast was now somewhat stronger and directed slightly more onshore. The 700-mb temperature at Annette dropped by 7 K; the thermal gradient between Yakutat and Annette was now small. The 0000 UTC 15 March sounding (released at approximately 2300 UTC on the 14th) from Yakutat (Fig. 3) shows weak static stability with respect to moist processes and near saturation from the surface to 650 mb. The wind profile reveals a low-level jet of 30 m s^{-1} at 850 mb.

Parameter values that characterize this case are an onshore velocity of 10 m s^{-1}, a static stability (calculated with respect to moist processes) of 7×10^{-3} s^{-1}, a Coriolis parameter of 1.2×10^{-4} s^{-1}, and a mountain height and half-width of 2000 m and 50 km, respectively. These values yield a Froude number of 0.7, a Rossby number of 1.7, a Rossby radius of 120 km, and a scaled terrain slope of 2.4. To summarize the synoptic situation, the southeastern coast of Alaska experienced moderate to strong southerly flow in the lower to middle troposphere and the passage of a frontal baroclinic zone, conditions that do not appear particularly unusual.

The influence of the terrain can be best seen from a series of sea level pressure analyses (Figs. 4a–e) at 3-h intervals between 1200 and 0000 UTC on the 15th. These analyses are essentially identical to the operational NMC analyses over the open Gulf of Alaska, but include significant differences in the coastal region. The analyses are subjective and are based on sparse data, but account for the effects of the coastal terrain in a consistent, dynamically plausible manner.

The analysis for 1200 UTC (Fig. 4a) shows a 994-mb low center near 55°N, 140°W and a surface front about 100 km off the coast. At 1500 UTC (Fig. 4b) the front was making landfall along the coast. The geostrophic flow behind the front was from the southwest (onshore) and of moderate intensity ($\sim$10 m s^{-1}). The pressure tendency analysis shows pressure falls of greater than 2 mb $(3\ h)^{-1}$ north of the low center and pressure rises of greater than 2 mb $(3\ h)^{-1}$ over the ocean south of the low and behind the front. The analysis for 1800 UTC (Fig. 4c) shows the low center about 150 km southwest of Yakutat with a central pressure of 992 mb. The front was passing over the rugged islands along the southeastern Alaska coast. Substantial ridging is shown behind the front from about Sitka (SIT) to about 300 km to the southeast. Within this region there were pressure rises of greater than 4 mb $(3\ h)^{-1}$, substantially greater than those analyzed behind the front while it was over the ocean. The wind at Sitka was from the south, suggesting that the mass and motion fields in this region had mutually adjusted toward a geostrophic balance. The wind was much more onshore at Langara Island (WLA) where the terrain is not as prominent. Sea level pressures had continued to fall behind the front north of about 58°N due to the northward propagation of the low center. The 2100 UTC analysis (Fig. 4d) shows the low center just to the southwest of Cape Yakataga (CYT) with the front having made landfall along its entire length. Pressure ridging continued along the coast, especially from Sitka to about 200 km to the northwest where pressure rises were greater than 4 mb $(3\ h)^{-1}$. Yakutat was now reporting southeast winds of 16 m s^{-1} with gusts to 28 m s^{-1} at the leading edge of the pressure rises behind the front. The analysis at 0000 UTC (Fig. 4e) shows the low center making landfall near 60°N, 145°W. The ridging along the coast and concomitant pressure rises greater than 4 mb $(3\ h)^{-1}$ were now situated over Yakutat, increasingly removed from the front. The stron-

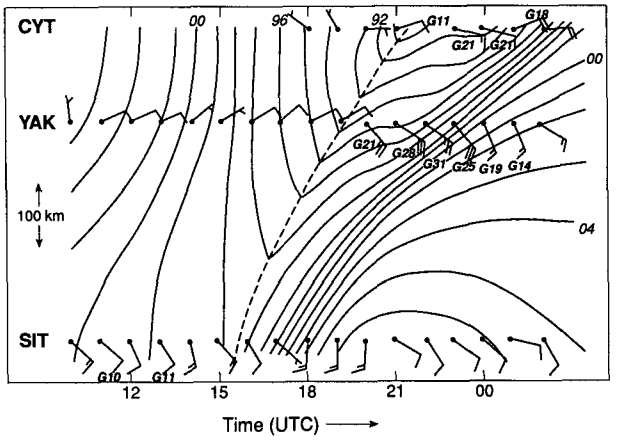

FIG. 5. Time section of sea level pressure (contours at 1-mb intervals) along the coastline of the Gulf of Alaska. The vertical scale is proportional to distance along the coast. Winds observed at Sitka, Yakutat, and Cape Yakataga are also plotted (full barb is 5 m s^{-1}; gusts in meters per second). The dashed line represents the front.

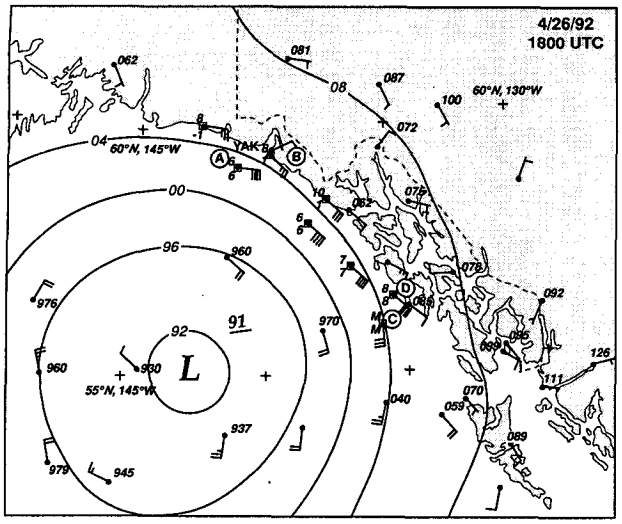

FIG. 6a. Sea level pressure (contours at 4-mb intervals) analysis for 1800 UTC 26 April 1992. Station pressures and winds are plotted in the conventional manner. Omega dropwindsonde (ODW) observations (950-mb winds, surface air temperatures, and dewpoints) are indicated by open boxes.

gest peak winds (21 m s^{-1}) were being reported at Cape Yakataga, again near the leading edge of the pressure rises along the coast.

Another perspective on this case is provided by a time section of sea level pressure and observed winds along the coast between Sitka and Cape Yakataga (Fig. 5). This plot shows the pressure falls ahead of the front and low pressure center, a 1–2-h period of pressure rises immediately behind the front, a 1-h period of suppressed pressure tendencies, and finally very large pressure rises surging up the coast increasingly behind the front. Both Yakutat and Cape Yakataga observed a 1-h period of zero pressure change behind the front but ahead of the pressure surge. The strongest winds occurred near the leading edge or just ahead of the surge, rather than in the region of the strongest alongshore pressure gradients. The surge moved up the coast at approximately 15 m s^{-1}.

b. Discussion

The severity of the winds near Yakutat can be attributed to the extreme low-level pressure gradients caused when a surge of pressure rises moved up the coast. It appears that this surge was a trapped feature that occurred along a hydrodynamically steep coastline. This phenomenon deserves a dynamical explanation.

The excess pressure rises that occurred along the coast (over those associated purely with the front) are presumably largely hydrostatic and caused by the pseudoadiabatic cooling within the air forced to rise over the terrain. This mechanism accounts for the barrier jets that have been observed along the upstream side of mountain ranges (e.g., Parish 1982). This case includes some of the aspects of a barrier jet, as evidenced by the low-level wind speed maximum in the Yakutat sounding (Fig. 3).

The time-dependent aspects of this case are less straightforward. The details of the pressure surge's structure cannot be completely determined from the available data but there are at least some resemblances with a solitary Kelvin wave. Its propagation speed of 15 m s^{-1} is close to the linear Kelvin wave speed of 14 m s^{-1} based on the estimated Rossby radius. The weather logs from Yakutat and Cape Yakataga do not indicate any type of sudden changes (on a scale of a few minutes) due to gravity–density current–like structure, but rather suggest that the transitions associated with the surge occurred over a period of 1–2 h. The speed of a gravity current can be related to a pressure difference across the density interface. Following Seitter and Muench (1985), and assuming the surge had a pressure perturbation of 3 mb, yields a propagation speed of approximately 12 m s^{-1}. Although this estimate is uncertain, the lack of any evidence of an abrupt transition, and the observations of strong winds ahead of the most rapid pressure rises, argue against a gravity current model for the surge. Most of the theoretical and observational work concerning coastally trapped Kelvin waves has involved the perturbations along an interface separating a two-layer system (e.g., Reason and Steyn 1992). The present case features a weakly continuously stratified fluid, which complicates extension of previous results.

It is interesting to speculate about what made this case unusual, since frontal cyclones are common in the Gulf of Alaska, and this one was not especially intense (Gray and Overland 1986). As mentioned above, the coastal ridging from Sitka southeastward occurred when the flow turned onshore behind the front. Yet this ridging occurred increasingly behind the front northwest of Sitka, despite similar geostrophic wind shifts at the front. The lack of pressure rises for a period behind the front is due at least in part to the synoptic pressure changes accompanying the northward-propagating low center. Perhaps the offshore-directed flow ahead of the front near Yakutat was significant in maintaining the intensity of the low center in the coastal zone. If the low center had been stationary, it is likely that the mesoscale pressure ridging would have been more synchronous along the coast, and the sea level pressure gradients near Yakutat would not have been as intense.

4. Two cases with ODW observations

The analysis of the Yakutat storm is hampered by the lack of observations in the nearshore region. ODW observations were collected along the Alaska coast on two other occasions when a synoptic low pressure system was present in the Gulf of Alaska. These observations are compared here with the coastal atmospheric structure for 14 March 1979.

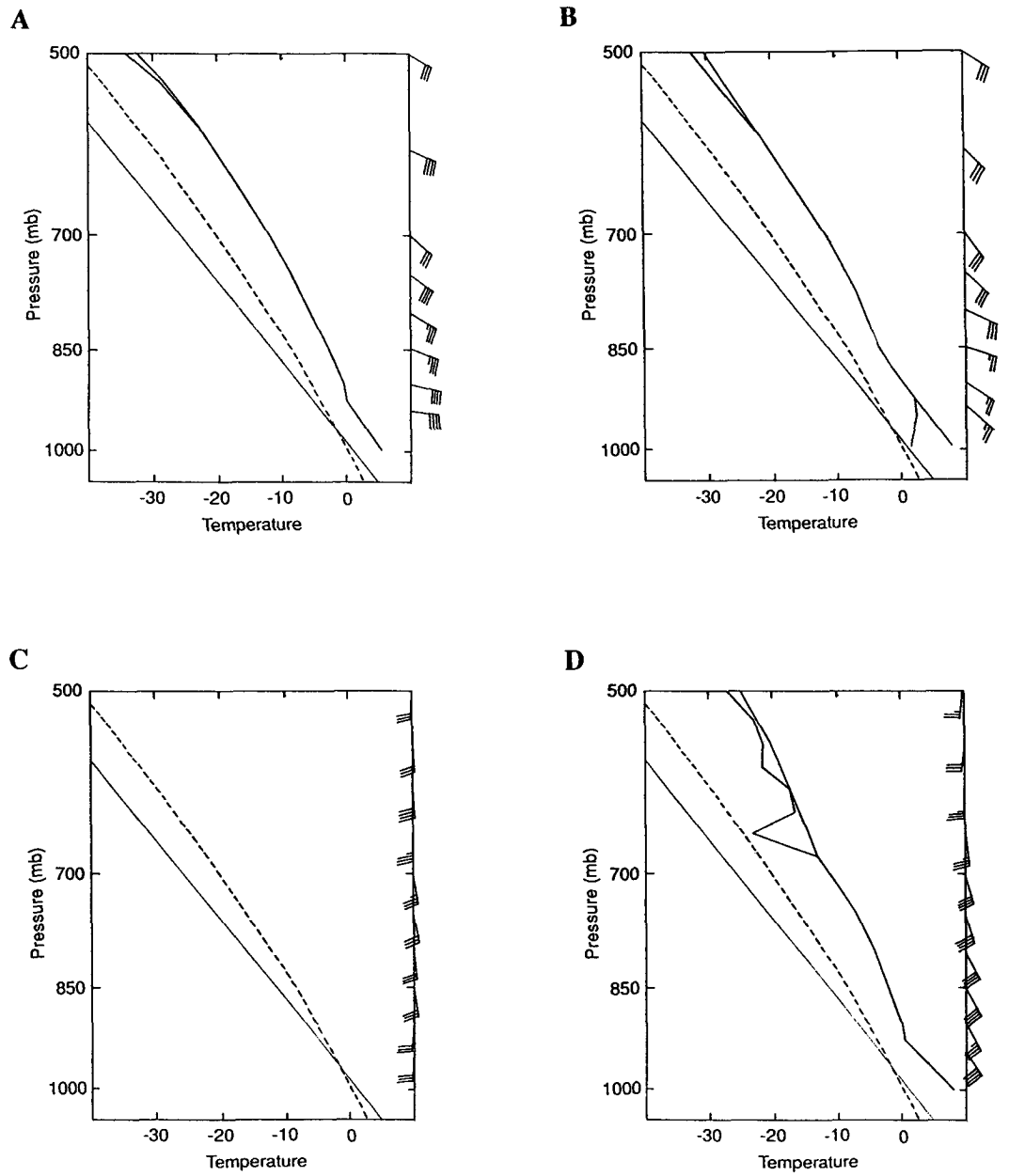

FIG. 6b. Selected ODW soundings plotted in the manner of Fig. 3; the locations of these soundings are indicated in Fig. 6a.

a. 26 April 1992

The sea level pressure analysis for 1800 UTC 26 April 1992 (Fig. 6a) shows a 991-mb low centered near 53°N, 142.5°W. This low was virtually stationary and slowly filling at this time. The surface geostrophic flow was directed predominantly along the entire southern and southeastern Alaskan coastline and was also slightly onshore south of 57°N. The 950-mb winds and surface air temperatures and dewpoints from the ODWs (identified by open boxes in Fig. 6a) along the coast are significantly different from those farther offshore. North of 58°N, it was warmer, drier, and less windy at the coast than at the locations of the soundings about 80 km offshore. Note the differences between the individual profiles plotted in A and B of Fig. 6b. South of 57°N, the single coastal sounding (profile D) showed saturation from the surface to 700 mb, and a stronger wind speed than the sounding farther offshore (profile C).

It appears that subsidence was occurring along the coast north of 58°N, as suggested by the low humidities

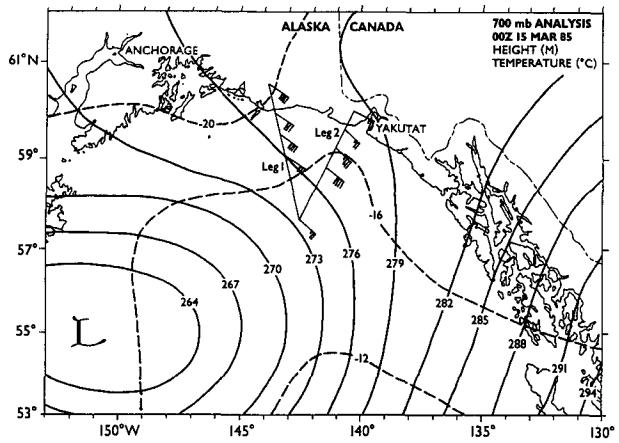

FIG. 7. 700-mb analysis at 0000 UTC 15 March 1985. The 700-mb winds from the ODW soundings are also plotted (full barb is 5 m s^{-1}).

from the coastal soundings and as further evidenced by the downslope surface flow at Yakutat. This subsidence, presumably maximized inland of the coast, would act to reduce the synoptically imposed pressure gradient right at the coast. On the other hand, the thermodynamic profile from the coastal ODW at location *D* (56.5°N, 135.2°W) suggests that rising motion was occurring along the coast south of 57°N where the low-level flow was slightly onshore. The cooling associated with the rising motion augments the large-scale pressure gradient and, hence, can account for the stronger winds observed at the coast than farther offshore. The ODW observations are insufficient to describe the details of the low-level structure near the coast. For example, they do not indicate how abrupt the transition was to the open ocean flow. Reynolds (1983) documented a frontlike feature at the leading edge of a katabatic outflow near Yakutat in somewhat similar synoptic conditions. There may have been a more gradual transition during the case of 26 April 1992 when the offshore-directed flow at the coast was warm. Our interpretation of the ODW observations is that the vertical motions associated with the coastal terrain induced mesoscale pressure perturbations, that is, the mechanism proposed for coastal ridging and enhanced alongshore coastal winds during the Yakutat storm of 14 March 1979.

b. 15 March 1985

The 700-mb analysis for 0000 UTC 15 March 1985 (Fig. 7) shows onshore-directed flow in the region of high-density ODW soundings west and southwest of Yakutat. The large-scale geostrophic flow at 850 mb (not shown) also had a significant onshore component. Significant baroclinity through warm-air advection is indicated offshore of southern Alaska. The mesoscale variations near the coast are better resolved in the summary of the ODW observations presented in Fig. 8. The 850-mb winds and geopotential heights from the soundings show that the 850-mb flow was essentially parallel to the coastal terrain. The strongest 850-mb winds observed were near the coast along leg 1 and about 100 km offshore along leg 2. The height gradients projected along axes normal to the 850-mb winds were slightly weaker along leg 1 than leg 2, even though the nearshore winds were stronger along leg 1. The 850-mb temperature gradients were weaker near the coast than farther offshore, yet the vertical wind shears between the 850- and 700-mb levels were generally larger near the coast. The mesoscale variations sampled in this dataset suggest that ageostrophic effects were important in the coastal zone. Yet it is difficult to isolate the influences of the terrain from the inherent thermal-wind properties of the synoptic storm system.

5. Conclusions

When synoptic-scale flow encounters coastal orography, mesoscale features are formed that have the scale of the half-width of broad coastal mountains or, more typically for steep mountains, have the scale of the Rossby radius based on mountain height. These scales of 50–150 km are smaller than observing networks, especially over water.

The Yakutat storm of 14 March 1979 and observations from 26 April 1992 and 15 March 1985 provide examples of coastal phenomena forced by time-depen-

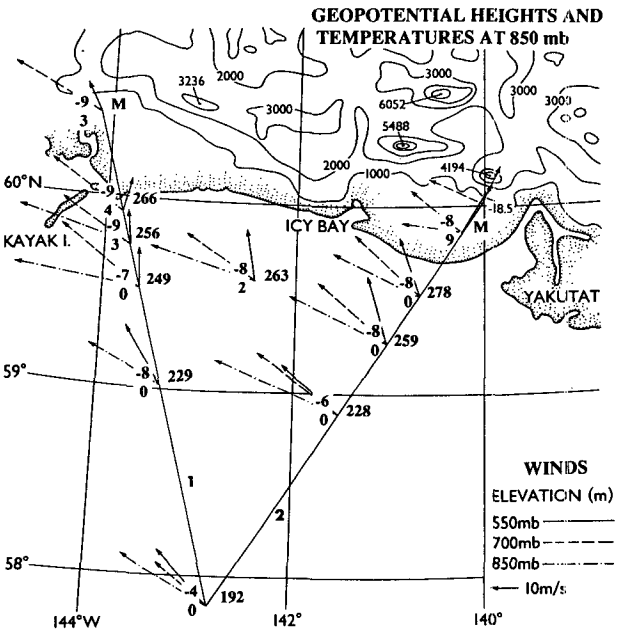

FIG. 8. Summary of ODW observations collected for the case of 15 March 1985. Wind vectors are plotted for the 550-, 700-, and 850-mb levels. 850-mb air temperatures, dewpoint depressions, and geopotential heights (meters above 1000 m) are also plotted to the left and right of the sounding locations, respectively.

dent synoptic flows in a region of prominent terrain. They include such features as damming, coastal propagation of a pressure wave, and offshore-directed leeside flow. Ageostrophic effects due to the orography are surmised to have been important in these cases, but even for the situation of 15 March 1985 when a high density of soundings was collected, these effects due to the terrain cannot be clearly segregated from the synoptic forcing. It would be useful to gather two sets of detailed observations in these kinds of situations, both before and after the storm becomes influenced by the terrain.

The dynamics of coastal phenomena are qualitatively known and local orographic forcing can be accounted for by specifying the finescale topography. In principle it is possible to forecast coastal winds based on the use of a regional numerical model driven by the larger synoptic-scale flow. It is critical that the models include the correct slope regimes, as in (6) rather than simply the correct maximum elevations. Further numerical and observational investigations of ageostrophic dynamics in the coastal zone are needed to improve conceptual and operational models. These studies will directly benefit forecasting of events such as the Yakutat storm, not only in southeastern Alaska, but also along other coastal regions with steep slopes.

Acknowledgments. Sections of this paper are an outgrowth of a chapter prepared for the National Academy of Sciences Panel on Coastal Meteorology; the contributions of the members of the panel are appreciated. Part of this material was presented at the Sixth Conference on Mountain Meteorology (sponsored by the American Meteorological Society) in Portland, Oregon. This paper is contribution 1351 from the Pacific Marine Environmental Laboratory of the National Oceanic and Atmospheric Administration and JISAO contribution 219.

REFERENCES

Bane, J. M., C. D. Winant, and J. E. Overland, 1990: Planning for coastal air–sea interaction studies in COPO. *Bull. Amer. Meteor. Soc.*, **71,** 514–519.

Beardsley, R. C., C. E. Dorman, C. A. Friehe, L. K. Rosenfeld, and C. D. Winant, 1987: Local atmospheric forcing during the coastal ocean dynamics experiment. 1. A description of the marine boundary layer and atmospheric conditions over a northern California upwelling region. *J. Geophys. Res.*, **92,** 1467–1488.

Bell, G. D., and L. F. Bosart, 1988: Appalachian cold-air damming. *Mon. Wea. Rev.*, **116,** 137–161.

Burger, A. P., 1991: The potential vorticity equation: From planetary to small scale. *Tellus,* **43,** 191–197.

Businger, S., and B. Walter, 1988: Comma cloud development and associated rapid cyclogenesis over the Gulf of Alaska: A case study using aircraft and operational data. *Mon. Wea. Rev.* **116,** 1103–1123.

Buzzi, A., and S. Tibaldi, 1978: A case study of Alpine lee cyclogenesis. *Quart. J. Roy. Meteor. Soc.*, **104,** 271–287.

Chen, W.-D., and R. B. Smith, 1987: Blocking and deflection of airflow by the Alps. *Mon. Wea. Rev.*, **115,** 2578–2597.

Colman, B. R., and C. F. Dierking, 1992: The Taku Wind of southeast Alaska: Its identification and prediction. *Wea. Forecasting,* **7,** 49–64.

Dorman, C. E., 1985: Evidence of Kelvin waves in California's marine layer and related eddy generation. *Mon. Wea. Rev.*, **113,** 827–839.

——, 1987: Possible role of gravity currents in northern California's coastal summer wind reversals. *J. Geophys. Res.*, **92,** 1497–1506.

Doyle, J. D., and T. T. Warner, 1991: A Carolina coastal low-level jet during GALE IOP 2. *Mon. Wea. Rev.*, **119,** 2414–2428.

Gray, J., and J. E. Overland, 1986: Meteorology. *Gulf of Alaska: Physical Environment and Biological Resources.* D. W. Hood and S. T. Zimmerman, Eds., U.S. Govt., 31–56.

Holland, G. J., and L. M. Leslie, 1986: Ducted coastal ridging over S.E. Australia. *Quart. J. Roy. Meteor. Soc.*, **112,** 731–748.

Mass, C. F., and M. D. Albright, 1987: Coastal southerlies and alongshore surges of the west coast of North America: Evidence of mesoscale topographically trapped response to synoptic forcing. *Mon. Wea. Rev.*, **115,** 1707–1738.

——, and G. K. Ferber, 1990: Surface pressure perturbations produced by an isolated mesoscale topographic barrier. Part 1: General characteristics and dynamics. *Mon. Wea. Rev.*, **118,** 2579–2596.

——, M. D. Albright, and D. J. Brees, 1986: The onshore surge of marine air into the Pacific Northwest: A coastal region of complex terrain. *Mon. Wea. Rev.*, **114,** 2602–2627.

National Research Council, 1992: *Coastal Meteorology.* National Academy Press, 99 pp.

Neiburger, M., 1960: The relation of air-mass structure to the field of motion over the eastern North Pacific Ocean in summer. *Tellus,* **12,** 31–40.

Overland, J. E., 1984: Scale analysis of marine winds in straits and along mountainous coasts. *Mon. Wea. Rev.*, **112,** 2530–2534.

Parish, T. R., 1982: Barrier winds along the Sierra Nevada mountains. *J. Appl. Meteor.*, **21,** 925–930.

Pierrehumbert, R. T., and B. Wyman, 1985: Upstream effects of mesoscale mountains. *J. Atmos. Sci.*, **42,** 977–1003.

Prandtl, L., 1936: Beiträge zur Mechanik der Atmosphäre. UGGI Assoc. Met. *Mem. et discussions,* 171–202.

Queney, P., 1948: The problem of airflow over mountains: A summary of theoretical studies. *Bull. Amer. Meteor. Soc.*, **29,** 16–26.

Reason, C. J. C., and D. G. Steyn, 1990: Coastally trapped disturbances in the lower atmosphere: Dynamic commonalities and geographic diversity. *Progr. in Phys. Geog.* **14,** 178–198.

——, and ——, 1992: The dynamics of coastally trapped mesoscale ridges in the lower atmosphere. *J. Atmos. Sci.*, **49,** 1677–1692.

Reynolds, M., 1983: Occurrence and structure of mesoscale fronts and cyclones near Icy Bay, Alaska. *Mon. Wea. Rev.*, **111,** 1938–1948.

Samelson, R. M., 1992: Supercritical marine-layer flow along a smoothly varying coastline. *J. Atmos. Sci.*, **49,** 1571–1584.

Schumann, U., 1987: Influence of mesoscale orography on idealized cold fronts. *J. Atmos. Sci.*, **44,** 3423–3441.

Seitter, K. L., and H. S. Muench, 1985: Observation of a cold front with a rope cloud. *Mon. Wea. Rev.*, **113,** 840–848.

Smith, R. B., 1979: The influence of mountains on the atmosphere. *Adv. Geophys.*, **21,** 87–230.

——, 1989: Hydrostatic airflow over mountains. *Adv. Geophys.*, **31,** 1–41.

Walter, B. A., and J. E. Overland, 1982: Response of stratified flow in the lee of the Olympic Mountains. *Mon. Wea. Rev.*, **110,** 1458–1473.

Winant, C. D., C. E. Dorman, C. A. Friehe, and R. C. Beardsley, 1988: The marine layer off northern California: An example of supercritical channel flow. *J. Atmos. Sci.*, **45,** 3588–3605.

Xu, Q., 1990: A theoretical study of cold air damming. *J. Atmos. Sci.*, **47,** 2969–2985.

Zemba, J., and C. A. Friehe, 1987: The marine atmospheric boundary layer jet in the coastal ocean dynamics experiment. *J. Geophys. Res.*, **92,** 1489–1496.